Vision-based Estimation of Slip Angle for Mobile Robots and Planetary Rovers

Giulio Reina, Genya Ishigami, Keiji Nagatani, and Kazuya Yoshida

***Abstract*— For a mobile robot it is critical to detect and compensate for slippage, especially when driving in rough terrain environments. Due to its highly unpredictable nature, drift largely affects the accuracy of localization and control systems, even leading, in extreme cases, to the danger of vehicle entrapment with consequent mission failure. This paper presents a novel method for lateral slip estimation based on visually observing the trace produced by the wheels of the robot, during traverse of soft, deformable terrain, as that expected for lunar and planetary rovers. The proposed algorithm uses a robust Hough transform enhanced by fuzzy reasoning to estimate the angle of inclination of the wheel trace with respect to the vehicle reference frame. Any deviation of the wheel trace from the expected pose, according to the direction of the robot's motion, suggests occurrence of sideslip that can be detected and, more interestingly, measured. This allows one to estimate the actual heading angle of the robot, usually referred to as the slip angle. The details of the various steps of the visual algorithm are presented and the results of experimental tests performed in the field with an all-terrain rover are shown, proving the method to be effective and robust.**

I. INTRODUCTION

The mobility of a robot driving across soft soils, such as sand, loose dirt, or snow, is greatly affected by the dynamic effects occurring at the wheel-terrain interface, such as slipping and skidding. As demonstrated by the Mars exploration of the NASA/JPL rovers Spirit and Opportunity [1], wheel slippage is a dominant disturbance on sandy slopes. This precludes the use of conventional dead-reckoning techniques for navigation, since they are based on the assumption that wheel revolutions can be translated into correspondent linear displacements. Thus, if one wheel slips, then the associated encoder will register revolutions even though these revolutions do not correspond to a linear displacement of the wheel. Conversely, if one wheel skids, fewer encoder pulses will be counted. Slippage not only affects the odometric accuracy, but increases the overall energy consumption and reduces the robot's traction and climbing performance. The availability of a sensory system able to estimate slip would be greatly beneficial to a mobile robot, so that its pose estimation could be compensated and corrective control actions may be executed, such as planning an alternate route away from a low-traction terrain region, or implementing a traction control algorithm [2]. Additionally, accurate position estimation is required for efficient and robust map building.

Most of the research in the field of mobile robotics has been focusing on the study of slip along the longitudinal direction of motion. Longitudinal slip can be estimated through the use of encoders by comparing the speed of driven wheels to that of undriven wheels [3]; however this does not apply for all-wheel drive vehicles or those without redundant encoders. Reina *et al* [4], proposed measures for slip detection, based on comparing different onboard sensor modalities within a fuzzy logic inference engine. Ojeda *et al* [5], presented a motor current-based slip estimator, while in [6], a Kalman filter-based approach combining encoders, IMU, and GPS was discussed for detecting immobilization conditions of a mobile robot. However, in the presence of side forces, the robot moves at an angle, usually referred to as slip angle, with respect to its longitudinal axis, resulting in lateral slip as well [7]. Thus, it is very important to address the issue of measuring the combined lateral and longitudinal slip. A large body of research work exists in the automotive community related to traction control, anti-lock braking systems (ABS), and electronic stability program (ESP). However, these works generally apply to asphalt roads and at significantly higher speeds than those typical for autonomous robots [8], [9]. In this area, Kalman filters have been widely applied to inertial and absolute measurements, such as GPS, to enhance dead reckoning and estimate lateral slip [10], [11]. However, GPS is not an option for planetary applications, nearby trees and buildings can cause signal loss and multipath errors, and changing satellites can cause position and velocity jumps [12]. Additionally, GPS provides low frequency updates (e.g. typically near 1 Hz) making GPS alone too slow for accurate slip detection.

This paper investigates the feasibility of a novel approach for slip angle estimation developed for mobile robots traveling on sandy terrain, such as that encountered by planetary rovers. The general approach is based on using a rear video camera to observe the pose of the trace that is produced by the wheels, and detect whether the robot follows the desired path or deviates from it because of slippage. Figure 1 shows a direct example that will help to clarify this approach, here proposed for the first time. For the extensive testing of the system during its development, we employed the rover El-Dorado, built at the Space Robotics Lab of the Tohoku University and shown in Fig. 1. The rear webcam, mounted to a frame attached to the vehicle's body, is visible in the same figure. Eldorado is an independently controlled 4-wheel-drive/4-wheel-steer mobile robot, also featuring a

This work was supported by the JSPS Fellowship program.

G. Reina is with the Department of Innovation Engineering, University of Salento, 73100 Lecce, Italy. Email: giulio.reina@unile.it

G. Ishigami, K. Nagatani, and K. Yoshida are with the Department of Aerospace Engineering, Tohoku University, Aoba 6-6-01, 980-8579 Sendai, Japan. Email: {ishigami, nagatani, yoshida}@astro.mech.tohoku.ac.jp

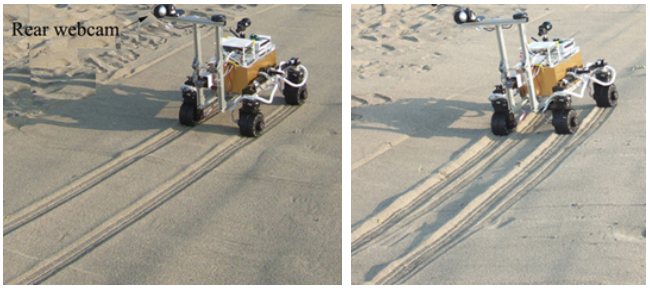

(a) (b)

Fig. 1. Sideslip estimation on sandy terrain by visual observation of the wheel traces with a rear webcam: (a) wheel traces parallel to the direction of motion, no lateral slip, (b) wheel traces inclined with respect to the intended direction of motion, significant lateral slip

typical rocker-type suspension system. Its operational speed ranges from 2 to 30 cm/s. The robot is equipped with wheel and steer encoders, a fluxgate compass to measure the absolute vehicle heading, a rear-mounted camera and other sensors such as laser range finder and GPS that are not employed for this application. Figure 1(a) shows El-Dorado as driving up a sandy slope following a straight path without any significant sideslip. This is shown by two distinct traces parallel to the direction of motion and produced by the wheel pair of either side of the robot. In Fig. 1(b), El-Dorado negotiates a sandy slope with a contemporary transverse inclination, as also shown by the slight roll angle of the robot. The consequent external side force acting on the rover results in a substantial lateral drift. The traces, left by the wheels of the same side of the robot, are no longer superimposed and, most importantly, their angle of inclination, with respect to a reference frame attached to the vehicle, differs from the case of absence of slip. The proposed approach aims at estimating the slip angle of the robot by measuring the pose of one of the wheel traces, i.e. the rear left wheel, in conjunction with the knowledge of its rate-of-turn provided by the onboard compass.

Somewhat related research has been devoted to the study of lane departure warning systems and automated highways. A wide variety of techniques has been employed aiming at developing efficient and robust lane detectors based on visually observing white road markings on dark and relatively uniform background [13], [14]. In previous research [15], a method for lane tracking was presented. In this paper a similar approach is extended and optimized for the special case of tracking wheel traces on sandy terrain. Since our approach is based on Hough transform supported by Fuzzy logic to provide robust and accurate tracking of the wheel Trace, we call it FTrace. The paper is organized as follows. Theoretical and experimental description of the FTrace module is provided in Section II. In Section III, the system is proved to be effective and robust in field tests performed with the rover El-Dorado. Section IV concludes this paper.

II. The FTrace system

Tracking the trace of a wheel can turn into a very complex problem especially when shadows, occlusions, and terrain unevenness come into play. A robust and efficient trace detection system must be able to filter out all disturbances and extract the marking of interest from a non-uniform background in order to produce an accurate and reliable estimate of the trace pose relative to the vehicle. In Fig. 2, a sample image set demonstrates the variety of terrain and environmental conditions that can be encountered. Figure 2(a) shows a scene where trace detection can be considered relatively easy thanks to the clearly defined imprint and uniform terrain texture. In Fig. 2(b), extraction of wheel trace is more difficult due to the presence of transverse line-like discontinuities of the terrain. Figure 2(c) shows a non-uniform terrain texture, whereas in Fig. 2(d) and Fig. 2(e) a more complex wheel trace is shown due to presence of heavy shadowing. Figure 2f refers to a scene where different imprints are present.

The FTrace module performs wheel trace tracking based on a robust Hough Transform enhanced by fuzzy logic. The relevant geometrical properties extracted from the scene are optimally combined based on in-depth physical understanding of the problem. In this section, a theoretical analysis of the method is presented providing also experimental evidences of its effectiveness.

A. Theoretical Analysis

1) Model Building: The presence of a rear camera mounted on the vehicle body is assumed, with a field of view on the ground plane corresponding to a 60 cm long $\times$ 80 cm wide area, behind the left rear wheel. It is also considered that the location of the camera relative to the wheel is known and fixed during travel. Under the assumption that the portion of the trace in the image, and the amount of sideslip, is relatively small between two consecutive frames, its curvature can be neglected and it is possible to refer to a trace model composed of a single line, corresponding to its centerline. In the image plane of the camera, the model pose is defined by the two polar parameters ρ, and φ as shown in Fig. 3. In the real world, we can refer to a simple schematic of the vehicle, known as the bicycle model [16], and shown in Fig. 4. The bicycle model neglects weight transfer from inner to outer tires and assumes the same tires and slip angles on the inner and outer wheels. The trace pose is defined by the distance d_t with respect to the center of mass of the vehicle G, and the angle θ_t between the velocity vector of the rear wheel V_r and the wheel longitudinal axis. This angle is also usually referred to as the slip angle of the wheel α_r. It is also assumed that the trace originates from the center of the wheel and thus it must always pass through the point B, as shown in Fig. 4. With reference to the same figure, we can also define the slip angle β of the vehicle as the angle between the velocity vector V of its center of mass G and the longitudinal axis X_v. Under the assumption of small angles, the following linearized relations hold between the

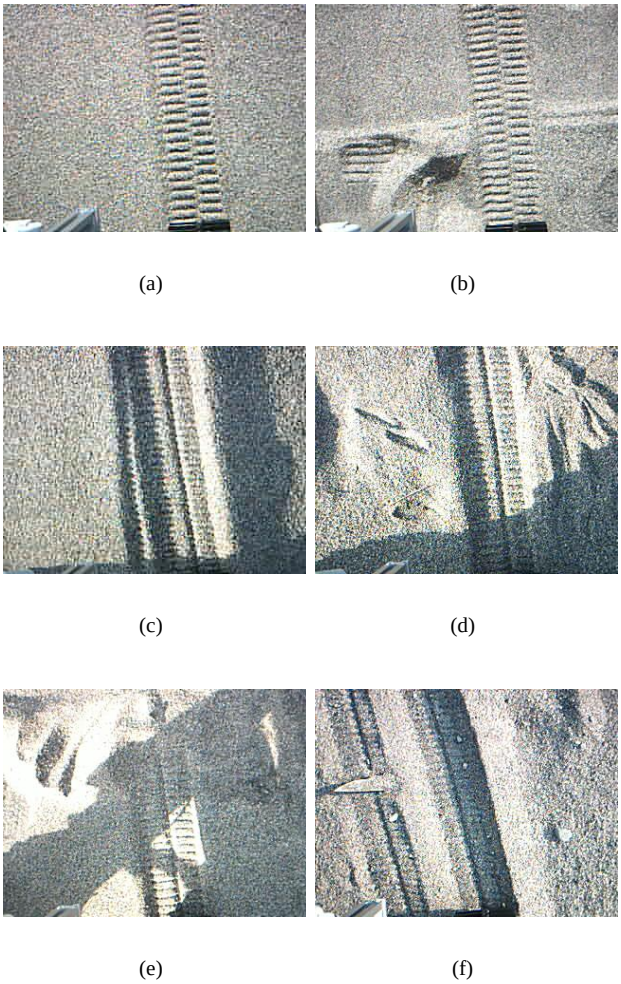

Fig. 2. Sample images of terrain and wheel trace conditions: (a) uniform sandy terrain, (b) disturbances due to transversal line-like discontinuities, (c) non-uniform terrain texture, (d) and (e) non-uniform terrain texture with noise due to shadowing, (f) different imprints present in the scene

slip angles and the velocity components

$$\beta = \frac{V_y}{V_x} \tag{1}$$

$$\alpha_r - \delta_r = \frac{V_y - r \cdot b}{V_x} = \beta - \frac{b}{R} \tag{2}$$

where V_x, V_y are the longitudinal and lateral component of the velocity vector V, δ_r is the rear steer angle, r is the rate-of-turn expressed in rad/s, R, defined as $R = V_x/r$, represents the distance of the instantaneous center of rotation from the longitudinal axis of the vehicle, and b is the distance between the rear axis and the center of mass G.
From (2), it is possible to estimate the slip angle β, given δ_r and V_x from the steer and wheel encoders, and r by differentiation from the onboard compass. Note, however, that the contribution of the term b/R is typically very small and practically β can be confused with α_r, when also δ_r is null.

2) Trace tracking: The FTrace module performs two main tasks:

- Extraction of trace candidates and estimation of their pose with respect to the camera, i.e. the vehicle, reference frame.
- Selection of the candidate that best fits to the trace model.

In the reminder of this section each phase is described in detail.

Trace extraction — Each image is processed following two steps. First, an optimized Canny's edge detection [17] is performed. Then, Hough transform [18], is applied to extract lines from the scene. Edges in images are areas with strong intensity contrasts. Edge detection significantly reduces the amount of data and filters out useless information, while preserving the important structural properties of the objects in the scene. The Canny's operator is based on a 3×3 Sobel kernel and the Low Threshold (LT) and High Threshold (HT) hysteresis were well determined experimentally as

$$LT = \frac{I_{max} - I_{min}}{3} \tag{3}$$

$$HT = 2.5 \cdot LT \tag{4}$$

where I_{max} and I_{min} are the maximum and minimum intensity value, respectively, detected in the current frame.
Ideally, edge detection is able to identify object boundaries. However, because of noise, non-uniform illumination, and other spurious effects, this technique usually fails to characterize edges completely. Hence, edge linking methods must

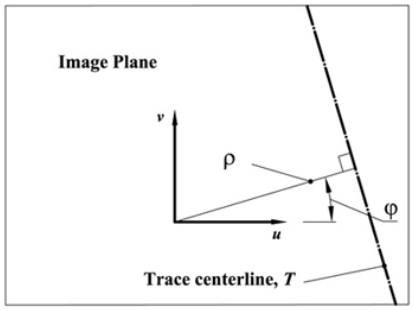

Fig. 3. Model of the trace of the wheel in the image plane. Note that the parameter ρ is expressed in pixels

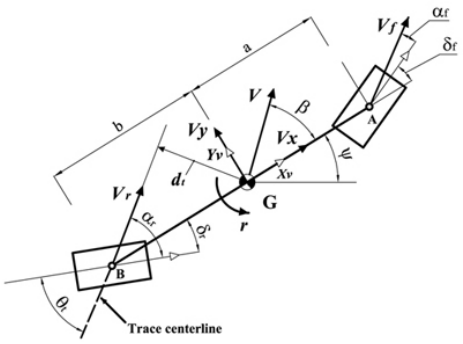

Fig. 4. Model of the trace in the real world with reference to a bicycle schematization of the robot

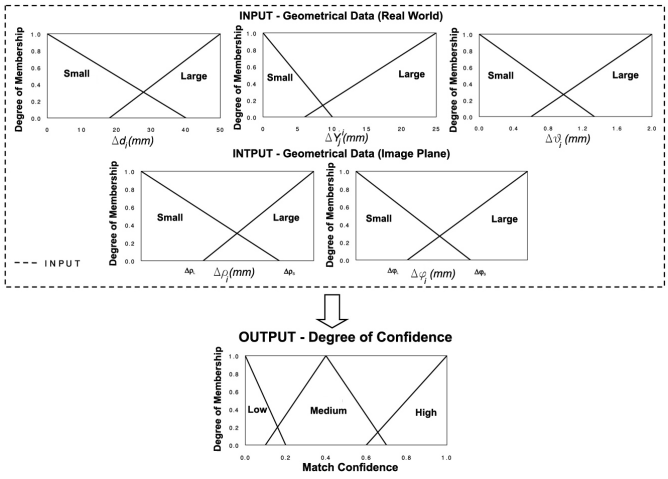

Fig. 5. Membership functions of the FTrace system

be used to assemble pixels into meaningful edges. One of the most known edge linking methods is the Hough transform that allows one to fit lines to the edges, detected by Canny's operator. At the end of the Hough transform application, a set of trace candidates will be available.

Trace selection — In order to determine which line best fits to the trace model we use fuzzy reasoning [19]. The general approach is based on comparing the geometrical properties of each candidate with those of the trace model, (as defined in Section II-A.1), in both the image plane and the real world, and defining deterministic conditions for model matching. The output of the FTrace is a fuzzy quantity that expresses the certainty that the line agrees exactly with the trace model.

Given n lines (e.g., n=10) extracted from the image i and generally denoted as T_j^i (e.g., j = 1, 2,.., n), one can compute their pose in the image plane $P_j^i = (\rho_j^i, \varphi_j^i)$, and compare it with that of the trace marker obtained in the previous frame $P^{i-1} = (\rho^{i-1}, \varphi^{i-1})$. Under the assumption of relatively small displacement of the trace with respect to the robot between two consecutive frames, P^{i-1} can be regarded as a good reference value. If the trace pose P_j^i agrees with P^{i-1}, then one can expect good correspondence between that line and the trace model. Poor correspondence suggests low likelihood of matching. Similarly, the pose of the trace candidate T_j^i in the real world $R_j^i = (d_j^i, \theta_j^i)$ can be compared with that estimated in the previous frame $R^{i-1} = (d^{i-1}, \theta^{i-1})$. Small change in the distance and orientation values suggests high likelihood of matching of the candidate with the model.

Finally, in the real world, the candidate T_j^i must also fulfill the geometrical constraint of passing through the center of the wheel, namely point B in Fig. 4. With reference to the same figure, one can compute the intersection Y_j^i of the candidate T_j^i with the parallel to the axis Y_v through point B, and the distance of Y_j^i from the center of the wheel as $\Delta Y_j^i = |Y_j^i - Y_B|$, where Y_B is the coordinate of B along Y_v. If the discrepancy is small, then one can expect good agreement with the model. Conversely, large values of ΔY_j^i suggest poor confidence of matching.

We express these hypotheses with fuzzy logic that uses rules to map from inputs to outputs. The triangular membership functions of the inference system are shown in Fig. 5. The fuzzy data fusion uses five inputs and one output. The inputs are the geometrical data, i.e., the absolute difference in distance and orientation estimated in the image plane, denoted with $\Delta\rho_j$ and $\Delta\varphi_j$ respectively, and in the real world, denoted with Δd_j and $\Delta\theta_j$ respectively, between the candidate pose and the model pose in the previous frame, and the distance ΔY_j^i of the candidate from the wheel center B. The output is a dimensionless factor, ranging from zero to one, which expresses the degree of confidence we have that the candidate matches the trace model. The fuzzy inference system fuses the geometrical information based on the *if-then* rule set shown in Table I. Those rules express our physical understanding of the phenomenon and they were chosen to give the best performance over other alternatives using a trial and error process. The rule set is not unique; new rules may be thought of and implemented to improve the output of the system.

B. Experimental Analysis

Representative experimental results of the FTrace are shown in Fig. 6 for a sample image where ten candidates were extracted by our system. Table II collects the confidence match for each one of the lines, as estimated by the FTrace module. As expected, the lane marker L_7 yields the greatest confidence level (87%), and is therefore selected as the best match. In Fig. 6(d), the output of the FTrace system is overlaid over the original scene along with the estimated values of d_t and θ_t.

III. Experimental Results

In this section experimental results are presented, aimed at assessing the overall effectiveness of the FTrace method. Tests were performed in the field using the rover El-Dorado, equipped with a cost-effective rear webcam, and a sampling rate of 5 Hz. The webcam was calibrated using the Matlab camera calibration toolbox [20]. The test field was located on the shoreline of a sandy beach, comprising large flat areas and sparse mounds of different extensions and heights. In all experiments, the rover was remotely controlled using a wireless joypad with a travel speed of about 8 cm/s. Two types of path were considered:

TABLE I
FUZZY LOGIC RULES USED BY THE FTRACE MODULE

Rule	Input:					Output:
#	$\Delta\rho_j$	$\Delta\varphi_j$	Δd_j	$\Delta\theta_j$	ΔY_j^i	Confidence Match
1	Small	Small	Small	Small	Small	High
2	Small	Large	Small	Large	Small	Med.
3	Large	Small	Large	Small	Large	Low
4	Large	Large	Large	Large	Large	Low
5	Large	Large	Small	Small	Large	Low
6	Small	Small	Large	Large	Small	Med.

TABLE II

DEGREE OF CONFIDENCE IN THE WHEEL TRACE CANDIDATES OF FIG. 6, AS DERIVED FROM THE FTRACE SYSTEM

Candidate Line #	L_1	L_2	L_3	L_4	L_5	L_6	L_7	L_8	L_9	L_{10}
Confidence Match %	2.1	1.1	70.4	81.7	24.3	75.4	87.0	10.3	18.7	20.2

- $Path$ A: straight-line path on sandy relatively flat terrain. These experiments were aimed at evaluating undue errors of the FTrace system incurred by low-slippage terrain.
- $Path$ B: straight-line path on non-flat terrain, including driving uphill or sideways on sandy slopes with substantial lateral slip.

The entire experimental area was within the range of a laser-based absolute positioning system that provided the ground-truth translational position (x, y, z) with respect to a global coordinate axes. The ground-truth sideslip angle of the robot β_g was estimated as the difference between the absolute vehicle heading direction ψ_l, derived by the laser position-measurement system, and the vehicle heading ψ, measured by the onboard compass

$$\psi_l = \arctan(\frac{\dot{y}}{\dot{x}}) \tag{5}$$

$$\beta_g = \psi_l - \psi \tag{6}$$

The FTrace system was tested over a total of 5016 images showing the results collected in Table III for both sets of experiments. The percentage of false positives, i.e. a trace marker detected when actually there is no trace marker, was less than 1%. Conversely, false negatives arise when the trace marker is present in the image but the system is not able to detect it at all and does not return any information. The percentage of false negatives was less than 3%. Finally, misidentifications refer to cases in which a trace marker is present in the image but the system fails in recognizing it properly and returns wrong information. In all tests, misidentifications were less than 2%. The system proved to be robust to disturbances due to heavy shadowing, non-uniform terrain texture, and the presence of overlapping imprints.

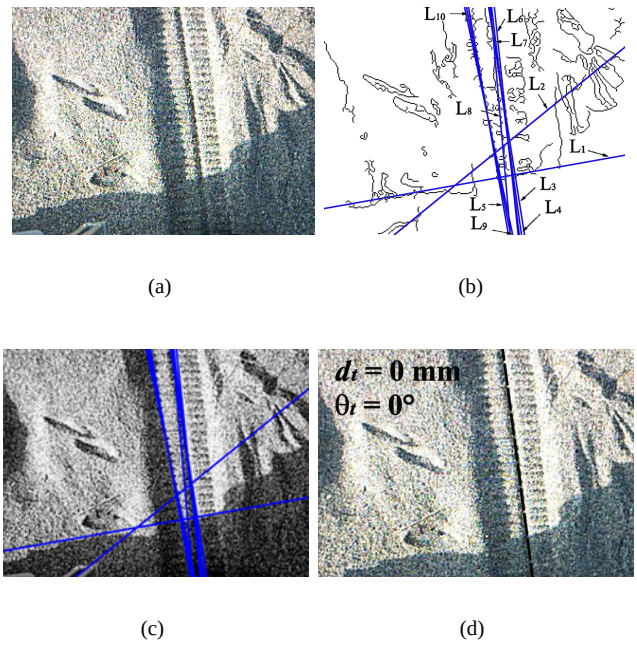

Fig. 6. Application of the FTrace system to a sample image: (a) original scene, (b) and (c) application of edge detection and Hough transform, (d) output of the FTrace system. Note that for this image no sideslip was detected

TABLE III

RESULTS OBTAINED FROM THE FTRACE SYSTEM FOR DIFFERENT TERRAINS. SET A: FLAT SANDY TERRAIN, SET B: NON-FLAT TERRAIN

Set #	Frames	False Positives (%)	False Negatives (%)	Misid.(%)
A	1560	0.0	1.5	0.0
B	3456	0.8	2.7	1.7

In order to assess the effectiveness of the FTrace system in estimating lateral drift, a typical test on non-flat terrain is presented. In this experiment, El-Dorado was commanded to move straight forward, driving sideways on a sandy slope resulting in a total travel distance of about D=7 m. Figure 7 shows the position of El-Dorado and the imprints produced by its wheels at the end of the run, from a front and rear view, respectively. In Fig. 8, the slip angle, derived from the FTrace system using (2), is compared with the ground-truth data. The two curves show good agreement with a root mean square (RMS) error less than 2 $\deg$. The FTrace system detected effectively the onset of sideslip and its successive trend throughout the experiment. Two different stages can be distinguished during the test. In the first stage referring to the first 60 seconds, the robot followed its intended straight path without any lateral drift. This is demonstrated by the two wheel traces parallel to the direction of motion. The second stage marks the onset of sideslip caused by the external lateral force acting on the rover due to the transverse inclination of the terrain. As direct consequence, a variation in the angle of inclination of the wheel traces is produced attesting to the occurrence of sideslip (see also Fig. 7). Since the accuracy of the FTrace method was consistent in all the experiments of both set A and B, this result can be regarded as of general significance.

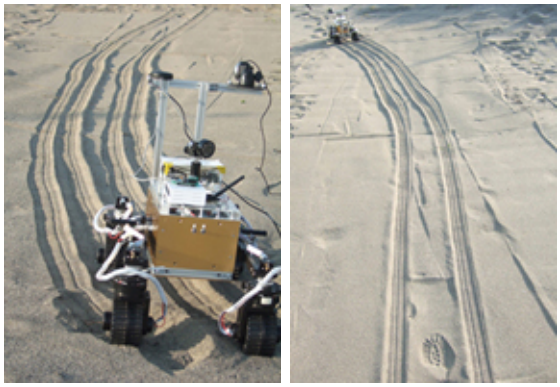

(a) (b)

Fig. 7. Traces produced by the wheels of the rover at the end of the traverse of a sandy slope: (a) front view, (b) rear view

IV. Conclusions

In this paper, a novel method for sideslip estimation was presented based on observing the wheel traces left by a robot during its traverse of sandy terrains. A visual algorithm was proposed to estimate the pose of the traces using Hough transform enhanced by fuzzy reasoning. The important geometrical data of the scene are combined based on the physical understanding of the problem providing accuracy and robustness. Comprehensive experiments in the field demonstrated the overall effectiveness of the proposed FTrace method for slip angle estimation on sandy terrain with a percentage of failed observations less than 2% and an accuracy of 1.4 deg. The FTrace module could be effectively employed to enhance the mobility of robots on highly challenging terrains by integration with conventional control and localization algorithm.

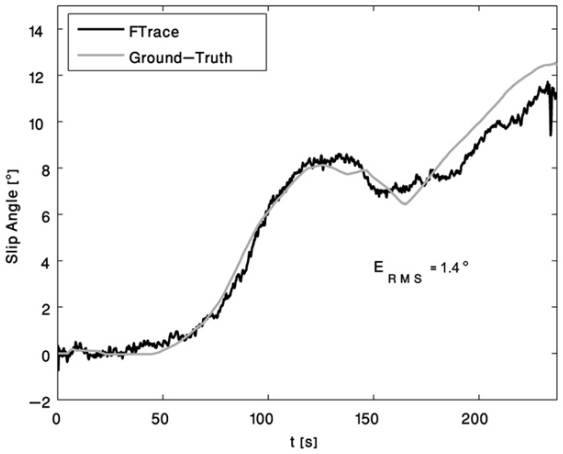

Fig. 8. Effectiveness of the FTrace system in estimating slip angle during sideways traverse of a sandy slope

V. Acknowledgments

The authors would like to thank the Japanese Society for the Promotion of Science for supporting the project through Fellowship P06061.

References

[1] M. Maimone, Y. Cheng, and L. Matthies, "Two Years of Visual Odometry on the Mars Exploration rovers," Journal of Field Robotics, vol. 24, no. 3, pp.169-186, 2007.
[2] T. Huntsberger et al., "Rover Autonomy for long Range Navigation and Science Data Acquisition on Planetary Surfaces," in Proc. IEEE Int. Conf. on Robotics and Automation, Washington, DC, 2002.
[3] F. Gustafsson, "Slip-based tire-road friction estimation," Automatica, vol. 33, no. 6, pp. 1087-1099, 1997.
[4] G. Reina, L. Ojeda, A. Milella, and J. Borenstein, "Wheel Slippage and Sinkage Detection for Planetary Rovers," IEEE/ASME Transactions on Mechatronics, vol. 11, no. 2, April, 2006.
[5] L. Ojeda, D. Cruz, G. Reina, J. Borenstein, "Current-based slippage detection and odometry correction for mobile robots and planetary rovers," IEEE Transactions on Robotics, vol. 22, no. 2, April 2006.
[6] C. Ward, and K. Iagnemma, "Model-based Wheel Slip Detection for Outdoor Mobile Robots," In Proc. IEEE Int. Conf. on Robotics and Automation, Rome, Italy, April 2007.
[7] G. Ishigami, A. Miwa, K. Nagatani, and K. Yoshida, "Terramechanics-based Model for Steering Maneuver of Planetary Exploration Rovers on Loose Soil," Journal of Field Robotics, vol. 24, no.3, pp.233-250, 2007.
[8] H. Tan, Y. Chin, "Vehicle antilock braking and traction control: a theoretical study," Int. J. of Systems Science, vol. 23, no. 3, 1992.
[9] Automotive Handbook, 5th ed., Robert Bosch GmbH, Germany, 2000.
[10] R. Anderson, D Bevly, "Estimation of slip angles using a model based estimator and GPS," In Proc. of American Control Conf., vol. 3, 2004.
[11] J. Hahn, R. Rajamani, L. Alexander,"GPS-based Real-Time Identification of Tire-Road Friction Coefficient," IEEE Transactions on Control Systems Technology, vol. 10, No. 3, May 2002.
[12] S. Sukkarieh, E. Nebot, H. Durrant-Whyte, "A high integrity IMU/GPS navigation loop for autonomous land vehicle applications," IEEE Trans. on Robotics and Automation, vol. 15, no. 3, June 1999.
[13] J.C. McCall and M.M. Trivedi, "Video-based Lane Estimation and Tracking for Driver Assistance: Survey, System, and Evaluation." IEEE Transactions on Intelligent Transportations Systems, Vol. 7, No.1, 2006.
[14] C. Taylor, J. Koeck, R. Blasi, and J. Malik, "A comparative study of vision-based lateral control strategies for autonomous highway driving," Int. J. Robot. Res., vol. 18, no. 5, pp. 442-453, May 1999.
[15] A. Milella, G. Reina, "A Fuzzy Lane Tracking System for Driver Assistance," Proc. ASME Int. Mechanical Engineering Congress and Exposition, Chicago, Usa, November 2006.
[16] G. Genta, Motor Vehicle Dynamics. World Scientific Publishing, Singapore, 2003.
[17] J. Canny, "A Computational Approach to Edge Detection," IEEE Transactions on Pattern Analysis and Machine Intelligence, Vol. 8, No. 6, 1986.
[18] P. Hough, "Methods and Means for Recognizing Complex Patterns", U.S. Patent, n. 3069654, 1962.
[19] J. M. Mendel, "Fuzzy Logic Systems for Engineering: A Tutorial," IEEE Proceedings, vol. 83, no. 3, 1995.
[20] J. Bouguet, "Camera Calibration Toolbox for Matlab," available on line at: http://www.vision.caltech.edu/bouguetj/calib_doc/